Development and *in vitro* evaluation of lipid nanoparticle-based dressings for topical treatment of chronic wounds

G. Gainza[1,2], W. S. Chu[3], R. H. Guy[3], J.L. Pedráz[1,2], R. M. Hernández[1,2], B. Delgado-Charro[3], M. Igartua[1,2,*]

[1] NanoBioCel Group, Laboratory of Pharmaceutics, School of Pharmacy, University of the Basque Country, Vitoria, Spain.

[2] Biomedical Research Networking Centre in Bioengineering, Biomaterials and Nanomedicine (CIBER-BBN), Vitoria, Spain.

[3] University of Bath, Department of Pharmacy & Pharmacology, Bath, UK

* Corresponding author

M. Igartua (manoli.igartua@ehu.es) and B. Delgado Charro (B.Delgado-Charro@bath.ac.uk) equally share credit for senior authorship.

Development and *in vitro* evaluation of lipid nanoparticle-based dressings for topical treatment of chronic wounds

ABSTRACT

This research addresses the development and *in vitro* evaluation of lipid nanoparticle (NP)-based dressings to optimize the delivery of human recombinant epidermal growth factor (rhEGF) for the topical treatment of chronic wounds. The systems investigated were rhEGF-loaded solid lipid nanoparticles (rhEGF-SLN) and rhEGF-loaded nanostructured lipid carriers (rhEGF-NLC) formulated in wound dressings comprising either semi-solid hydrogels or fibrin-based solid scaffolds. Following detailed characterisation of the NP, *in vitro* diffusion cell experiments (coupled with dermatopharmacokinetic measurements), together with confocal microscopic imaging, conducted on both intact skin samples, and those from which the barrier (the *stratum corneum*) had been removed, revealed that (a) the particles remained essentially superficially located for at least up to 48 hours post-application, (b) rhEGF released on the surface of intact skin was unable to penetrate to the deeper, viable layers, and (c) sustained release of growth factor from the NP "drug reservoirs" into barrier-compromised skin was observed. There were no significant differences between the *in vitro* performance of rhEGF-SLN and rhEGF-NLC, irrespective of the formulation employed. It is concluded that, because of their potentially longer-term stability, the fibrin-based scaffolds may be the most suitable approach to formulate rhEGF-loaded lipid nanoparticles.

Keywords: EGF (epidermal growth factor), wound dressing, lipid nanoparticles, skin, *stratum corneum*, Solid Lipid Nanoparticles, Nanostructured Lipid Carriers.

Abbreviations: Nanoparticle (NP), rhEGF-loaded solid lipid nanoparticles (rhEGF-SLN), rhEGF-loaded nanostructured lipid carriers (rhEGF-NLC), *stratum corneum* (SC), Epidermal growth factor (EGF), encapsulation efficiency (EE), occlusion factor (F), Polydispersity indices (PDI), laser scanning confocal microscopy (LSCM), Nile red (NR), 16-NBD palmitic acid (16-NBD).

1. INTRODUCTION

The skin is an attractive route for the administration of drugs intended for both local and systemic effects (Campbell, et al. 2012). In particular, the topical route for local treatment lowers the risk of systemic side effects, because the *stratum corneum* (SC), the most superficial skin layer, provides a significant barrier to drug penetration (Curdy, et al. 2004). Given that nanoparticles (NP) larger than 10 nm are unable to penetrate either intact or partially impaired skin to any great extent (Campbell, et al. 2012; Prow, et al. 2011), novel drug delivery systems for local effect based on this technology have been proposed as topical reservoirs from which the sustained release of an active compound may be achieved over a prolonged period of time. These characteristics support a strategy, therefore, of using biodegradable, drug-loaded nanoparticles for the topical treatment of skin disease-associated lesions and chronic wounds.

The administration of growth factors, such as epidermal growth factor (EGF), to accelerate wound healing has been extensively described (Choi, et al. 2008; Chu, et al. 2010; Gainza, et al. 2013; Hardwicke, et al. 2008; Hori, et al. 2007; Johnson and Wang 2013), however, topical delivery of EGF is severely limited by its high molecular weight, hydrophilicity and, above all, its short half life at the wound site (Al Haushey, et al. 2010; Choi, et al. 2012; Ulubayram, et al. 2001). To address these shortcomings, the nano-encapsulation of growth factors, like EGF, may enhance their stability at the wound and may allow their controlled release, thereby optimising efficacy. In this regard, the *in vivo* performance of topically applied recombinant human EGF (rhEGF)-loaded solid lipid nanoparticles (rhEGF-SLN) and nanostructured lipid carriers (rhEGF-NLC) in a superficially wounded animal model has been reported (Gainza, et al. 2014).

The topical administration of a NP-based delivery system may be facilitated by their incorporation into either semi-solid hydrogels or solid scaffolds. Bioadhesive hydrogels (e.g., Noveon® AA-1 polycarbophil, a high molecular weight polymer of acrylic acid chemically cross-linked with divinyl glycol) are widely used as wound dressings and their prolonged residence time in the skin offers the opportunity for sustained drug release (Ceschel, et al. 2001; Padamwar, et al. 2011). Semisolid hydrogels can be prepared using amphiphilic surfactants, such as Pluronic F-127 (Poloxamer 407), the reversible thermo-gelling behaviour of which creates an extremely versatile material for drug delivery (Antunes, et al. 2011; El-Kamel 2002; Kant, et al. 2014). Solid scaffolds, such as fibrin-based biomaterials with slow degradation kinetics, have also been frequently used as immune-compatible polymeric dressings from which drug delivery can be controlled (Briganti, et al. 2010; Moura, et al. 2014). A further advantage of this approach is that fibrin is an important haemostatic

mediator acting as a matrix for tissue repair, providing support for new capillaries, and generating an array of cell signalling compounds and growth factors following an injury (Brown and Barker 2014).

The present work aimed to further advance the development of local therapies with rhEGF. For this, the previously developed rhEGF-SLN and rhEGF-NLC (Gainza, et al. 2014) were embedded in three different vehicles Noveon® AA-1 hydrogels, Pluronic F-127 hydrogels and fibrin-based solid scaffolds proposed as potential wound dressings. The performance of these integrated wound dressing-delivery systems was characterized and compared to that of the corresponding nanoparticles suspension. This allowed investigating whether incorporation of the nanoparticles into semi-solid hydrogels and fibrin scaffolds modified the rate and extent of rhEGF release as well as the nanoparticle disposition through intact and partially damaged skin. Finally, we aimed to establish whether their hypothetical role of these systems as drug reservoirs for topical therapies could be demonstrated.

2. MATERIALS AND METHODS

2.1 Chemicals

Precirol® ATO 5 was from Gattefossé (Nanterre, France); Noveon® AA-1 Polycarbophil, USP, was purchased from Lubrizol (Barcelona, Spain); Pluronic F127, fibrinogen from bovine plasma, and thrombin, also from bovine plasma, were acquired from Sigma-Aldrich, Chemie GmbH (Steinhelm, Germany); Nile Red (analytical grade) was obtained from Sigma-Aldrich (St. Louis, MO, USA), 16-NBD palmitic acid from Avanti Polar Lipids, Inc. (Alabaster, AL, USA), and rhEGF was supplied by the Center for Genetic Engineering and Biotechnology, Cuba.

2.2 Skin

Dorsal, full-thickness porcine skin was obtained post-sacrifice from locally sourced female pigs. The skin was cleaned under cold running water and the subcutaneous fat was removed with a scalpel. The remaining tissue was then dermatomed to a thickness of ~750 μm and stored frozen at -20°C for up to at most one month before use.

2.3 Lipid nanoparticle (NP) preparation

rhEGF-SLN and rhEGF-NLC were prepared as previously described (Gainza, et al. 2014). Briefly, rhEGF-SLN were obtained by emulsifying 1% w/v Tween® 80 in milliQ water with an organic phase comprising 0.1% (w/v) rhEGF and 5% (w/v) Precirol® ATO 5 in dichloromethane using a 30 s period of sonication at 50 W (Branson® 250 Sonifier, CT, USA). The resulting emulsion was then

vigorously stirred for 2 h to evaporate the organic solvent. Subsequently, the rhEGF-SLN were collected by centrifugation/filtration at 2500 rpm for 10 minutes using a filter with a 100 kDa pore size (Amicon® Ultra, Millipore, Spain), and washed three times with milliQ water. Finally, particles were freeze-dried using trehalose (15% w/w of the lipid weight) as a cryoprotectant.

rhEGF-NLC were prepared at 40ºC by adding an aqueous solution of 0.67% w/v Poloxamer and 1.33% w/v Polysorbate 80 to a lipidic blend of melted Precirol® ATO 5 (200 mg) and Miglyol® 182 (20 mg). Subsequently, 100 µl of rhEGF in milliQ water (20 mg/ml) were added to the aqueous/lipidic mixture, which was then emulsified with sonication for 15s at 50 W. The resulting emulsion was stored for 12 h at 4ºC to allow lipid re-crystallisation and NLC formation. Finally, particles were collected, washed and freeze-dried as previously described.

In the experiments examining the disposition of the nanoparticles on the skin, the lipid phase of the formulations was labelled with two fluorophores: Nile Red (0.5% w/w of the lipid weight) and 16-NBD-palmitic acid (1% w/w of the lipid weight).

2.4 Preparation of wound dressings

For the hydrogel based wound dressings, either (a) rhEGF-SLN or rhEGF-NLC particles containing 20 µg of protein were added to an aqueous solution of 1% w/w Noveon® AA-1 and the dispersion was neutralised with triethanolamine to induce polymer gelation (Figure 1), or (b) a 30 % w/w Pluronic F-127 aqueous solution (prepared with vigorous stirring for 24 h at 4ºC) was added to a water suspension of rhEGF-SLN or rhEGF-NLC, again containing 20 µg of protein, and the mixture was stirred for 10 min, before being left at room temperature for 2 min to allow gel formation (Figure 1).

For the fibrin-based wound dressings, 5 mg of fibrinogen in 0.4 ml milliQ water at 37ºC and 0.1 ml of an aqueous dispersion of rhEGF-SLN and rhEGF-NLC (with 20 µg of protein) such that the final fibrinogen concentration was 10 mg/ml. Subsequently, 50 U/ml of thrombin were added and the resulting fibrin gel was freeze-dried to obtain the solid scaffold (Figure 1).

2.5 Nanoparticle characterisation

The nanoparticles in the formulations were characterised (Zetasizer Nano ZS, Malvern Instruments, Worcestershire, UK) in triplicate by their mean size (z-average), polydispersity index (PDI), and zeta potential (ζ). The pH of the reconstituted NP suspension, and of the NP-loaded Noveon® AA-1 and Pluronic F-127 hydrogels was also measured (Crison micropH 2001, Crison Instruments, S.A., Barcelona, Spain).

150 The encapsulation efficiency (EE) of rhEGF was determined indirectly by measuring the
151 concentration of free protein removed in the filtration/centrifugation step described in section 2.3.
152 The rhEGF assay used a commercially available sandwich enzyme-linked immunosorbent kit
153 (Human EGF ELISA Development Kit, Peprotech, London, UK). EE was expressed as the
154 percentage of the encapsulated rhEGF relative to the total amount used in the nanoparticle
155 preparation. All measurements were performed in triplicate, and the results reported as the mean ±
156 S.D.

157 *2.6 Rheological studies*

158 The rheological behaviour of the reconstituted NP suspensions, and of the Noveon® AA-1 and
159 Pluronic F-127 hydrogels, was characterised at 25ºC using an Advanced Rheometer (AR 1000, TA
160 Instruments, New Castle, USA) with a Peltier plate (17 mm diameter and 4 mm gap) for temperature
161 control. Measurements on 1 ml samples were made in triplicate at 0.5, 1, 2.5 and 5 rpm.

162 *2.7 Occlusivity test*

163 The protocol for this *in vitro* test was adapted from one previously described (Souto, et al. 2004).
164 Franz cells were filled with 5 ml of water and covered with a cellulose membrane (D9652,
165 MWCO~12,000, Sigma-Aldrich, Madrid, Spain). 5 mg of NP in the reconstituted suspensions, the
166 Noveon® AA-1 and Pluronic F-127 hydrogels, and the fibrin scaffold were applied to the exposed
167 surface of the cellulose membrane and the system was maintained at 32ºC for 48 h. Water loss from
168 the Franz cell was determined gravimetrically and compared to that when no formulation was
169 applied to the membrane. An occlusion factor (F) was calculated from the results using the following
170 equation:

171 $$F = \frac{\text{Water loss without formulation} - \text{Water loss with formulation}}{\text{Water loss without formulation}} x100$$

172 *2.8 In vitro drug release*

173 Vertical Franz diffusion cells (area = 1 cm^2) and cellulose membranes (MWCO~12,000, avg. flat width
174 33 mm, D9652, Sigma-Aldrich) as above were used. The receptor chamber was filled with 5 ml of
175 30% v/v ethanol in PBS and magnetically stirred. 0.5 ml of the formulations (containing 20 µg of
176 rhEGF) were spread on the exposed membrane surface in the donor chamber, which was sealed with
177 a layer of petrolatum gauze (Tegaderm®, 3M, St. Paul, MN, USA) to mimic a practical application.
178 Release of the active was measured over one week at 32ºC, 0.5 ml samples of the receptor solution
179 being taken (and replaced with an equal volume of fresh medium) over time. The rhEGF released
180 was measured by ELISA (n=3).

181 *2.9 Penetration of rhEGF into stratum corneum*

182 Before the experiments, skin was thawed and any large hairs were carefully trimmed. The skin
183 sample was clamped in a vertical Franz cell with a diffusion area of 3.14 cm^2 and the receptor
184 chamber was filled with 8 ml of milliQ water. The NP formulations (the Noveon® AA-1 and
185 Pluronic F-127 hydrogels, the fibrin-based scaffold, and the reconstituted NP suspension) were
186 applied to the skin and the donor chamber and sealed using Tegaderm® film. A suspension of free
187 rhEGF (20 µg in 0.5 ml of milliQ water) acted as a control. Experiments (n = 3) were carried out
188 for 48 h at 32ºC. The diffusion cells were then disassembled and the skin cleaned with wet tissue.
189 A plastic template was applied to delimit a constant area, which was repetitively stripped with 12
190 adhesive tapes (Tesafilm® 5529, Beiersdorf, Hamburg, Germany) of area 0.5 cm^2. The {tapes +
191 *stratum corneum*} were placed into vials and rhEGF was extracted with 1 ml of 0.05% Tween-20
192 and 0.1% BSA in PBS under a gentle agitation for 17 h. The first 4 tapes were extracted individually
193 while tapes 5-12 were treated together as the protein concentration therein was expected to be much
194 lower. A few (3 – 5) tape-strips were also taken from untreated skin and acted as controls. The
195 extracted rhEGF was measured by ELISA.

196 *2.10 Uptake of rhEGF into damaged skin*

197 Skin was first tape-stripped (Tesafilm® 5529) 20 times to substantially undermine its barrier
198 function as measured by transepidermal water loss (Aquaflux, Biox Systems Ltd., London, UK).
199 The uptake and permeation of rhEGF from the various NP formulations through the compromised
200 skin was determined as before in Franz diffusion cells. Post-treatment and surface cleaning, rhEGF
201 was extracted from the entire skin into 4 ml of 0.05% Tween-20 and 0.1% BSA in PBS. A control
202 experiment was performed using intact skin and a 40 µg/ml suspension of rhEGF in milliQ water
203 as the donor.

204 *2.11 Penetration of rhEGF into skin from fluorescently-labeled NP formulations*

205 These experiments were conducted as described in section 2.10 for 6, 24 and 48 h with formulations
206 labeled with either Nile Red or 16-NBD-palmitic acid. The damaged skin was then examined by
207 laser scanning confocal microscopy (510 Meta inverted confocal laser scanning microscope, Carl
208 Zeiss, Jena, Germany). The samples were excited sequentially using argon (excitation line 488 nm,
209 green) and HeNe (excitation line 543 nm,red) lasers; a Plan-Neofluar 40×/1.30 oil objective (DIC
210 M27, Carl Zeiss, Jena, Germany) was used for acquisition of all images. Fluorescence signals were
211 recorded at 505–530 nm (green) for the 16-NBD-palmitic acid labelled formulations and at 560 nm

(red) for the Nile Red labeled formulations. Confocal images (xy-plane) were obtained every 2 µm in the z-direction parallel to the sample surface.

3. RESULTS AND DISCUSSION

3.1. rhEGF-SLN and rhEGF-NLC characterisation, rheological studies and occlusion tests.

The topical disposition of nanoparticles is related to particle size and skin integrity (Jensen, et al. 2011; Müller, et al. 2002). For instance, particles larger than 10 nm in diameter appear unable to penetrate either intact or partially impaired skin (Campbell, et al. 2012; Prow, et al. 2011). The research described in this paper aims to explore whether rhEGF-loaded lipid nanoparticles are suitable platforms for the local treatment of chronic wounds, an objective best served (it is believed) by large enough particles to prolong residence time at the injury site and to avoid or minimize systemic uptake. Table 1 shows that all the nanoparticles studied in this work were similar in size (320-350 nm in diameter) and not expected, therefore, to penetrate the skin, whether neither intact or damaged. Polydispersity indices (PDI) were less than 0.5 and zeta potentials were approximately -30 to -20 mV; hence, the particles could be considered relatively monodisperse and stable against coalescence (Aznar, et al. 2013; Kuchler, et al. 2009). The encapsulation efficiencies were 95 (±3.59) % and 74 (±1.39)% for the rhEGF-NLC and rhEGF-SLN, respectively. The higher EE of the former is probably a reflection of the amorphous structure of NLC particles that minimizes drug expulsion during the encapsulation process; these results are in agreement with those described previously (Gainza, et al. 2014; Pardeike, et al. 2009).

The pH values of the NP formulations fell within the 4-7 range recommended for topical products (Duncan, et al. 2013) (Table 2). The rheology and occlusivity results show that rhEGF-SLN and rhEGF-NLC had similar properties (Table 2). As expected, all hydrogels had significantly higher viscosities ($p < 0.05$) than the suspensions, suggesting that the former would have an increased residence time at a wound site and permit the prolonged release of rhEGF.

The SLN-based suspensions and the integrated wound dressing-delivery systems were more occlusive than those prepared with NLC (Table 2), possibly because the SLN lipid matrix impedes water evaporation more than the semisolid NLC (Mandawgade and Patravale 2008). The fibrin-based scaffolds were the most occlusive. No differences in occlusivity were found between the two hydrogel-based formulations. In other words, it appears that it is solely the nature of the lipid film formed on the skin by the NP, which confers occlusive properties to the formulations. This characteristic is particularly relevant because it increase skin hydration and thus allows the sustained release of drugs (Souto, et al. 2004).

3.2. In vitro drug release

The release profiles of rhEGF from the reconstituted NP suspensions and from the integrated wound dressing-drug delivery systems are depicted in Figure 2. As expected, rhEGF was released faster and in a greater extent (~80%) from the aqueous suspensions of the nanoparticles than from the integrated wound dressing-delivery systems ($p < 0.05$). When the nanoparticles were incorporated into the hydrogel formulations, there is an additional barrier to rhEGF release (Hu, et al. 2005) (relative to that from the aqueous dispersions), which is markedly retarded for the first 4 days. Drug release from hydrogel formulations is reported to depend primarily on the polymer concentration, degree of crosslinking and mesh size, as well as the hydrophilicity and molecular weight of the active compound (Amsden 1998; Hamidi, et al. 2008). It is noted that blends of polymeric hydrogels (such as Noveon® AA-1 or Pluronic F-127) and lipid nanoparticles can manifest higher viscosity conferred by strong intermolecular forces and thereby liberate an encapsulated drug more slowly (Antunes, et al. 2011). Despite the similar viscosities of the hydrogels, the concentration of Pluronic F-127 used is 30-fold higher than that of Noveon® AA-1 and this may explain the slower rhEGF release from the former (for example, 20% rhEGF released after 7 days from F-127 compared to 30% from Noveon®.

The fibrin-based wound dressings released more rhEGF than the hydrogels. The difference was significant throughout the study with respect to the Pluronic F-127, but only at 2 and 4 days compared with the Noveon® AA-1 hydrogel ($p < 0.05$). However, rhEGF release from the fibrin-based scaffolds was less than that from the reconstituted NP suspensions, supporting the potential of these platforms for controlled drug delivery. Fibrin also represents a useful model for the extracellular matrix by stabilising growth factors and promoting healing (Briganti, et al. 2010; Losi, et al. 2013; Oju Jeon, et al. 2005).

3.3. Penetration of rhEGF into stratum corneum

Uptake of rhEGF from the various formulations into the *stratum corneum* (SC) was assessed by tape-stripping after a 48 h exposure. All the NP-based formulations (whether with SLN or NLC, the performance of which were very similar) resulted in greater uptake of rhEGF into the SC than treatment with a simple solution of the protein (Table 3), even though release from the integrated wound dressing-drug delivery systems was far from complete in this time period (as discussed above see Figure 2). However, regardless of the formulation, most of the rhEGF taken up into the SC was constrained to the skin surface, i.e., was resident on the first tape-strip (Figure 3A), with very little retrieved from the subsequent 11 strips (Figure 3B). Taken together, these results imply that there is minimal, if any, movement of rhEGF from the intact skin surface into the deeper SC (Al Haushey,

et al. 2010; Almeida and Souto 2007). The presence of the protein in tape-strips 2-12 is most likely a reflection of formulation which has been incompletely removed from 'furrows' in the skin surface, or hair follicle openings, by the cleaning procedure performed prior to tape-stripping (Lademann, et al. 2005). Nonetheless, the retention of the delivery systems on the skin surface is a positive feature (the fibrin-based scaffolds were particularly substantive and difficult to remove) that points to their potential to sustain drug release over time when the barrier is absent or compromised (as was examined in the subsequent series of experiments now discussed).

3.4. Uptake of rhEGF into damaged skin

The uptake of rhEGF from the formulations examined into skin samples from which the SC had been essentially removed prior to dosing is shown in Table 3. The recovery of the protein was higher from all the wound dressing-drug delivery systems, and from the reconstituted NP suspensions, than that from damaged skin treated with free rhEGF in solution, suggesting that associating the protein with nanoparticles had a positive effect on drug stability (Gokce, et al. 2012; Magdassi 1997; Schäfer-Korting, et al. 2007). For each type of wound dressing considered (i.e., the two hydrogels and the fibrin scaffolds), the uptake of rhEGF was independent of the type of lipid used (SLC or NLC). Protein uptake was highest from the simple NP suspensions, presumably due to the faster release of drug relative to that from the hydrogel and fibrin-based systems. With respect to the latter, protein recovery from the skin from the Noveon hydrogel and the fibrin scaffold was similar and slightly better than that from the Pluronic-based formulations probably explained by the greater polymer concentration and the slower release (see discussion above) (Antunes, et al. 2011). It was again observed that the fibrin vehicles adhered particularly well to the skin suggesting that this formulation may be able to prolong rhEGF residence time at the wound site.

3.5. Penetration of rhEGF into skin from fluorescently-labeled NP formulations

Laser scanning confocal microscopy (LSCM) is a non-invasive imaging technique for the study of the skin disposition and penetration of labeled nanoformulations which permits the direct imaging of the fluorescent target at different depths without any mechanical sectioning (Alvarez-Román, et al. 2004a; Alvarez-Román, et al. 2004b). In this study, SLN and NLC were labeled first with Nile Red (NR), a lipophilic compound that was encapsulated into the NP. The potential limitation of NR is that it can be released from the NP, dye the skin and give unreal information of the NP penetration. For this reason, 16-NBD palmitic acid (16-NBD), a fluorescent lipid, which labels the NP directly, was used to give an accurate localization of NP in the skin. In this regard, the LSCM study also seeks to investigate the differences between labeling NP with NR or 16-NBD palmitic acid.

LSCM and reflectance images of barrier-impaired skin samples treated for 6, 24 and 48 hours with the labeled SLN and NLC formulations were recorded (Figures 4-5). With respect to the nanoparticles, whose disposition was monitored by 16-NBD fluorescence, no differences were observed as a function of time: the particles were only found at the skin surface and did not migrate further into the tissue during the treatment period (a finding in complete agreement with a recent study that demonstrated the inability of 20-200 nm NP to penetrate beyond the superficial layer of the SC even when the skin was partially damaged by tape stripping (Campbell, et al. 2012). No influence of the vehicle was apparent.

For the NP applied as a suspension and in the Noveon® AA-1 hydrogel, the release of the NR and its subsequent penetration into the deeper skin layers was apparent (illustrated with the white circle in Figure 5). This observation is consistent with the rhEGF skin uptake results discussed above and with data from earlier work, which used NR as a model active to probe drug delivery from topically applied nanoparticles (Alvarez-Román, et al. 2004a; Alvarez-Román, et al. 2004b). In contrast, NR penetration into the skin from either the Pluronic F-127 hydrogel or the fibrin scaffold was not detectable (Figure 5). For the Pluronic, this result confirms the earlier deduction that this hydrogel provides an additional barrier to limit release of the 'active' (Amsden 1998; Hamidi, et al. 2008). In the case of the nanoparticle-loaded fibrin scaffolds, the extent of NR release was difficult to visualize because the reflectance images of the fibrin layer and of the skin were very similar. As a result, and exacerbated by the strong interaction/adhesion between the fibrin scaffold and the skin, it was impossible to define with any accuracy the location of the interface between the two. Nonetheless, it may reasonably be anticipated that, in the environment of a typical open wound, the fibrin scaffold would be slowly and progressively hydrolyzed and able to liberate the drug-loaded NP *in situ*.

4. CONCLUSIONS

Lipidic nanoparticles, loaded with rhEGF and gelled in appropriate vehicles are potentially useful formulations for the local treatment of chronic wounds. Independent of the vehicle chosen, the NP are constrained to the surface while acting, over at least a 48 hour period as reservoirs to sustain release of the protein. A combination of *in vitro* release, dermatopharmacokinetic and partially damaged skin uptake experiments revealed no significant difference between the drug delivery performance of SLN and NLC. In terms of the formulation, fibrin-based scaffolds were perceived to have advantageous (relative to commercially available gels) both in terms of their improved shelf-life and their biocompatible, haemostatic properties. Further *in vivo* work, as well as longer-term stability measurements, are required to confirm this potential.

Acknowledgements

G. Gainza was funded by a fellowship from the University of the Basque Country (UPV/EHU). The project was supported in part by the Basque and the Spanish Governments (Consolidated Groups, IT-407-07 and INNPACTO, IPT-2012-0602-300000, 2012, respectively). Additional support from the University of the Basque Country UPV/EHU (UFI11/32) and the University of Bath (UK) is gratefully acknowledged.

REFERENCES

Al Haushey, L., Bolzinger, M.A., Fessi, H., Briancon, S., 2010. rhEGF microsphere formulation and in vitro skin evaluation. J. Microencapsul., 27, 14-24. doi: 10.3109/02652040902749061; 10.3109/02652040902749061.

Almeida, A.J., Souto, E., 2007. Solid lipid nanoparticles as a drug delivery system for peptides and proteins. Adv. Drug Deliv. Rev., 59, 478-490. doi: http://dx.doi.org/10.1016/j.addr.2007.04.007.

Alvarez-Román, R., Naik, A., Kalia, Y.N., Fessi, H., Guy, R.H., 2004a. Visualization of skin penetration using confocal laser scanning microscopy. Eur. J. Pharm. Biopharm, 58, 301-316. doi: http://dx.doi.org/10.1016/j.ejpb.2004.03.027.

Alvarez-Román, R., Naik, A., Kalia, Y.N., Guy, R.H., Fessi, H., 2004b. Skin penetration and distribution of polymeric nanoparticles. J. Control. Release, 99, 53-62. doi: http://dx.doi.org/10.1016/j.jconrel.2004.06.015.

Amsden, B., 1998. Solute Diffusion within Hydrogels. Mechanisms and Models. , 31, 8382-8395.

Antunes, F.E., Gentile, L., Oliviero Rossi, C., Tavano, L., Ranieri, G.A., 2011. Gels of Pluronic F127 and nonionic surfactants from rheological characterization to controlled drug permeation. Colloids and Surfaces B: Biointerfaces, 87, 42-48. doi: http://dx.doi.org/10.1016/j.colsurfb.2011.04.033.

Aznar, M.Á., Lasa-Saracíbar, B., Estella-Hermoso de Mendoza, A., Blanco-Prieto, M.J., 2013. Efficacy of edelfosine lipid nanoparticles in breast cancer cells. Int. J. Pharm., 454, 720-726. doi: http://dx.doi.org/10.1016/j.ijpharm.2013.04.068.

Briganti, E., Spiller, D., Mirtelli, C., Kull, S., Counoupas, C., Losi, P., Senesi, S., Di Stefano, R., Soldani, G., 2010. A composite fibrin-based scaffold for controlled delivery of bioactive pro-angiogenetic growth factors. J. Control. Release, 142, 14-21. doi: http://dx.doi.org/10.1016/j.jconrel.2009.09.029.

Brown, A.C., Barker, T.H., 2014. Fibrin-based biomaterials: Modulation of macroscopic properties through rational design at the molecular level. Acta Biomater., 10, 1502-1514. doi: http://dx.doi.org/10.1016/j.actbio.2013.09.008.

Campbell, C.S.J., Contreras-Rojas, L.R., Delgado-Charro, M.B., Guy, R.H., 2012. Objective assessment of nanoparticle disposition in mammalian skin after topical exposure. J. Control. Release, 162, 201-207. doi: http://dx.doi.org/10.1016/j.jconrel.2012.06.024.

Ceschel, G.C., Maffei, P., Lombardi Borgia, S., Ronchi, C., 2001. Design and evaluation of buccal adhesive hydrocortisone acetate (HCA) tablets. Drug Deliv., 8, 161-171. doi: 10.1080/107175401316906937.

Choi, J.S., Leong, K.W., Yoo, H.S., 2008. *In vivo* wound healing of diabetic ulcers using electrospun nanofibers immobilized with human epidermal growth factor (EGF). Biomaterials, 29, 587-596. doi: 10.1016/j.biomaterials.2007.10.012.

Choi, J.K., Jang, J., Jang, W., Kim, J., Bae, I., Bae, J., Park, Y., Kim, B.J., Lim, K., Park, J.W., 2012. The effect of epidermal growth factor (EGF) conjugated with low-molecular-weight protamine

(LMWP) on wound healing of the skin. Biomaterials, 33, 8579-8590. doi: http://dx.doi.org/10.1016/j.biomaterials.2012.07.061.

Chu, Y., Yu, D., Wang, P., Xu, J., Li, D., Ding, M., 2010. Nanotechnology promotes the full-thickness diabetic wound healing effect of recombinant human epidermal growth factor in diabetic rats. Wound Repair Regen., 18, 499-505. doi: 10.1111/j.1524-475X.2010.00612.x; 10.1111/j.1524-475X.2010.00612.x.

Curdy, C., Naik, A., Kalia, Y.N., Alberti, I., Guy, R.H., 2004. Non-invasive assessment of the effect of formulation excipients on *stratum corneum* barrier function in vivo. Int. J. Pharm., 271, 251-256. doi: http://dx.doi.org/10.1016/j.ijpharm.2003.11.016.

Duncan, C.N., Riley, T.V., Carson, K.C., Budgeon, C.A., Siffleet, J., 2013. The effect of an acidic cleanser versus soap on the skin pH and micro-flora of adult patients: A non-randomised two group crossover study in an intensive care unit. Intensive and Critical Care Nursing, 29, 291-296. doi: http://dx.doi.org/10.1016/j.iccn.2013.03.005.

El-Kamel, A.H., 2002. In vitro and in vivo evaluation of Pluronic F127-based ocular delivery system for timolol maleate. Int. J. Pharm., 241, 47-55. doi: http://dx.doi.org/10.1016/S0378-5173(02)00234-X.

Gainza, G., Aguirre, J.J., Pedraz, J.L., Hernández, R.M., Igartua, M., 2013. rhEGF-loaded PLGA-Alginate microspheres enhance the healing of full-thickness excisional wounds in diabetised Wistar rats. Eur. J. Pharm. Sci., 50, 243-252. doi: http://dx.doi.org/10.1016/j.ejps.2013.07.003.

Gainza, G., Pastor, M., Aguirre, J.J., Villullas, S., Pedraz, J.L., Hernandez, R.M., Igartua, M., 2014. A novel strategy for the treatment of chronic wounds based on the topical administration of rhEGF-loaded lipid nanoparticles: In vitro bioactivity and in vivo effectiveness in healing-impaired db/db mice. J. Control. Release, 185, 51-61. doi: http://dx.doi.org/10.1016/j.jconrel.2014.04.032.

Gokce, E.H., Korkmaz, E., Dellera, E., Sandri, G., Bonferoni, M.C., Ozer, O., 2012. Resveratrol-loaded solid lipid nanoparticles versus nanostructured lipid carriers: evaluation of antioxidant potential for dermal applications. Int. J. Nanomedicine, 7, 1841-1850. doi: 10.2147/IJN.S29710; 10.2147/IJN.S29710.

Hamidi, M., Azadi, A., Rafiei, P., 2008. Hydrogel nanoparticles in drug delivery. Adv. Drug Deliv. Rev., 60, 1638-1649. doi: http://dx.doi.org/10.1016/j.addr.2008.08.002.

Hardwicke, J., Schmaljohann, D., Boyce, D., Thomas, D., 2008. Epidermal growth factor therapy and wound healing--past, present and future perspectives. Surgeon, 6, 172-177.

Hori, K., Sotozono, C., Hamuro, J., Yamasaki, K., Kimura, Y., Ozeki, M., Tabata, Y., Kinoshita, S., 2007. Controlled-release of epidermal growth factor from cationized gelatin hydrogel enhances corneal epithelial wound healing. J. Control., 118, 169-176. doi: DOI: 10.1016/j.jconrel.2006.12.011.

Hu, F., Jiang, S., Du, Y., Yuan, H., Ye, Y., Zeng, S., 2005. Preparation and characterization of stearic acid nanostructured lipid carriers by solvent diffusion method in an aqueous system. Colloids and Surfaces B: Biointerfaces, 45, 167-173. doi: http://dx.doi.org/10.1016/j.colsurfb.2005.08.005.

425 Jensen, L.B., Petersson, K., Nielsen, H.M., 2011. In vitro penetration properties of solid lipid
426 nanoparticles in intact and barrier-impaired skin. Eur. J. Pharm. Biopharm., 79, 68-75. doi:
427 http://dx.doi.org/10.1016/j.ejpb.2011.05.012.

428 Johnson, N.R., Wang, Y., 2013. Controlled delivery of heparin-binding EGF-like growth factor
429 yields fast and comprehensive wound healing. J. Control. Release, 166, 124-129. doi:
430 http://dx.doi.org/10.1016/j.jconrel.2012.11.004.

431 Kant, V., Gopal, A., Kumar, D., Gopalkrishnan, A., Pathak, N.N., Kurade, N.P., Tandan, S.K.,
432 Kumar, D., 2014. Topical pluronic F-127 gel application enhances cutaneous wound healing in rats.
433 Acta Histochem., 116, 5-13. doi: http://dx.doi.org/10.1016/j.acthis.2013.04.010.

434 Kuchler, S., Abdel-Mottaleb, M., Lamprecht, A., Radowski, M.R., Haag, R., Schafer-Korting, M.,
435 2009. Influence of nanocarrier type and size on skin delivery of hydrophilic agents. Int. J. Pharm.,
436 377, 169-172. doi: 10.1016/j.ijpharm.2009.04.046; 10.1016/j.ijpharm.2009.04.046.

437 Lademann, J., Weigmann, H.J., Schanzer, S., Richter, H., Audring, H., Antoniou, C., Tsikrikas, G.,
438 Gers-Barlag, H., Sterry, W., 2005. Optical investigations to avoid the disturbing influences of
439 furrows and wrinkles quantifying penetration of drugs and cosmetics into the skin by tape stripping.
440 J. Biomed. Opt., 10, 054015. doi: 10.1117/1.2055507.

441 Losi, P., Briganti, E., Errico, C., Lisella, A., Sanguinetti, E., Chiellini, F., Soldani, G., 2013. Fibrin-
442 based scaffold incorporating VEGF- and bFGF-loaded nanoparticles stimulates wound healing in
443 diabetic mice. Acta Biomater., 9, 7814-7821. doi: http://dx.doi.org/10.1016/j.actbio.2013.04.019.

444 Magdassi, S., 1997. Delivery systems in cosmetics. Colloids Surf. Physicochem. Eng. Aspects, 123–
445 124, 671-679. doi: http://dx.doi.org/10.1016/S0927-7757(97)03792-8.

446 Mandawgade, S.D., Patravale, V.B., 2008. Development of SLNs from natural lipids: application to
447 topical delivery of tretinoin. Int. J. Pharm., 363, 132-138. doi: 10.1016/j.ijpharm.2008.06.028;
448 10.1016/j.ijpharm.2008.06.028.

449 Moura, L.I.F., Dias, A.M.A., Suesca, E., Casadiegos, S., Leal, E.C., Fontanilla, M.R., Carvalho, L.,
450 de Sousa, H.C., Carvalho, E., 2014. Neurotensin-loaded collagen dressings reduce inflammation and
451 improve wound healing in diabetic mice. Biochimica et Biophysica Acta (BBA) - Molecular Basis of
452 Disease, 1842, 32-43. doi: http://dx.doi.org/10.1016/j.bbadis.2013.10.009.

453 Müller, R.H., Radtke, M., Wissing, S.A., 2002. Solid lipid nanoparticles (SLN) and nanostructured
454 lipid carriers (NLC) in cosmetic and dermatological preparations. Adv. Drug Deliv. Rev., 54,
455 Supplement, S131-S155. doi: 10.1016/S0169-409X(02)00118-7.

456 Oju Jeon, Soo Hyun Ryu, Ji Hyung Chung, Kim, B., 2005. Control of basic fibroblast growth factor
457 release from fibrin gel with heparin and concentrations of fibrinogen and thrombin. J. Control.
458 Release, 105, 249-259. doi: http://dx.doi.org/10.1016/j.jconrel.2005.03.023.

459 Padamwar, M.N., Patole, M.S., Pokharkar, V.B., 2011. Chitosan-reduced gold nanoparticles: a novel
460 carrier for the preparation of spray-dried liposomes for topical delivery. J. Liposome Res., 21, 324-
461 332. doi: 10.3109/08982104.2011.575380; 10.3109/08982104.2011.575380.

462 Pardeike, J., Hommoss, A., Muller, R.H., 2009. Lipid nanoparticles (SLN, NLC) in cosmetic and
463 pharmaceutical dermal products. Int. J. Pharm., 366, 170-184. doi: 10.1016/j.ijpharm.2008.10.003;
464 10.1016/j.ijpharm.2008.10.003.

465 Prow, T.W., Grice, J.E., Lin, L.L., Faye, R., Butler, M., Becker, W., Wurm, E.M.T., Yoong, C.,
466 Robertson, T.A., Soyer, H.P., Roberts, M.S., 2011. Nanoparticles and microparticles for skin drug
467 delivery. Adv. Drug Deliv. Rev., 63, 470-491. doi: http://dx.doi.org/10.1016/j.addr.2011.01.012.

468 Schäfer-Korting, M., Mehnert, W., Korting, H., 2007. Lipid nanoparticles for improved topical
469 application of drugs for skin diseases. Adv. Drug Deliv. Rev., 59, 427-443. doi:
470 http://dx.doi.org/10.1016/j.addr.2007.04.006.

471 Souto, E.B., Wissing, S.A., Barbosa, C.M., Muller, R.H., 2004. Development of a controlled release
472 formulation based on SLN and NLC for topical clotrimazole delivery. Int. J. Pharm., 278, 71-77. doi:
473 10.1016/j.ijpharm.2004.02.032.

474 Ulubayram, K., Cakar, A.N., Korkusuz, P., Ertan, C., Hasirci, N., 2001. EGF containing gelatin-
475 based wound dressings. Biomaterials, 22, 1345-1356. doi: DOI: 10.1016/S0142-9612(00)00287-8.

476

Nanoparticle formulation	Mean size (nm)	PDI.	ζ- potential (mv)	EE (%)
rhEGF-SLN	330.77 ± 3.59	0.22 ± 0.02	-27.20 ± 0.44	74.22 ± 1.39
rhEGF-NLC	343.07 ± 5.90	0.21 ± 0.04	-20.30 ± 0.36	95.06 ± 3.59
NileRed-SLN	323.97 ± 2.86	0.40 ± 0.02	-29.30 ± 0.22	-
NileRed-NLC	345.60 ± 13.28	0.41 ± 0.01	-28.97 ± 2.90	-
16-NBC-palmitic acid-SLN	327.30 ± 3.64	0.36 ± 0.03	-28.03 ± 0.12	-
16-NBC-palmitic acid-NLC	333.70 ± 7.35	0.42 ± 0.05	-30.60 ± 1.59	-

Formulation	pH	Viscosity at 1 rpm (Pa·s)	Occlusion factor (f)
rhEGF-SLN suspension	5.88 ± 0.03	0.03 ± 0.00	24.26 ± 1.19
rhEGF-NLC suspension	5.83 ± 0.01	0.03 ± 0.01	15.91 ± 0.18
rhEGF-SLN Noveon® AA-1	5.07 ± 0.04	18.86 ± 0.19	36.05 ± 7.04
rhEGF-NLC Noveon® AA-1	5.04 ± 0.04	16.51 ± 2.81	22.64 ± 2.81
rhEGF-SLN Pluronic F-127	6.18 ± 0.04	24.70 ± 6.57	33.10 ± 3.20
rhEGF-NLC Pluronic F-127	6.26 ± 0.02	22.27 ± 6.10	21.46 ± 2.44
rhEGF-SLN fibrin based scaffold	-	-	48.33 ± 9.22
rhEGF-NLC fibrin based scaffold	-	-	41.05 ± 4.43

FORMULATION	% of administrated dose	
	SC - Intact skin	Skin - Barrier impaired
Free rhEGF	1.45 ± 0.08	0.60 ± 0.04
rhEGF-SLN suspension	9.78 ± 0.59 [a]	14.66 ± 1.62 [c]
rhEGF-SLN Noveon® AA-1	7.31 ± 0.45	9.34 ± 1.40 [d]
rhEGF-SLN Pluronic F-123	4.87 ± 0.06	4.77 ± 0.28 [b]
rhEGF-SLN fibrin based scaffold	14.55 ± 1.74 [a]	10.26 ± 1.91 [d]
rhEGF-NLC suspension	10.49 ± 1.64 [a]	15.63 ± 2.73 [c]
rhEGF-NLC Noveon® AA-1	5.38 ± 0.52	8.68 ± 2.03 [b]
rhEGF-NLC Pluronic F-123	4.27 ± 0.57	5.94 ± 0.76 [b]
rhEGF-NLC fibrin based scaffold	11.04 ± 1.76 [a]	9.37 ± 1.58 [b]

Figure captions

Table 1: Physicochemical characterization of the formulations: nanoparticle diameter, polydispersity index (PDI), zeta potential and encapsulation efficiency (EE). Data shown are mean ± S.D. (n = 3).

Table 2: pH, viscosity and occlusion factor of the formulations tested. Data shown are mean ± S.D. (n = 3).

Table 3: rhEGF recovery from the SC (12 tapes) following intact skin permeation experiments and from the skin following barrier-impaired skin permeation experiments. Data shown as mean ± S.D.). Intact skin: [a] significantly greater than free rhEGF ($p<0.05$, one-way ANOVA). Barrier impaired skin: [b.] significantly greater than Free rhEGF. [c] significantly greater than Free rhEGF, Noveon® AA-1 hydrogels, Pluronic F-123 hydrogels and Fibrin-based scaffolds. [d] significantly greater than Free rhEGF and Pluronic F-127 hydrogels ($p<0.05$, one-way ANOVA).

Figure 1: rhEGF-SLN and rhEGF-NLC integrated wound dressing – delivery systems: Noveon® AA-1 hydrogel, Pluronic F-127 hydrogel, fibrin-based scaffold, and reconstituted NP suspension.

Figure 2: *In vitro* release profiles of rhEGF from (A) SLN, and (B) NLC formulations. Data shown are mean ± S.D. (n = 3).

Figure 3: rhEGF uptake into intact *stratum corneum* treated with a control solution of the protein, reconstituted NP suspensions, and integrated wound dressing-drug delivery systems. Amounts of rhEGF recovered in the first tape-strip (Panel A) and on tape-strips 2-12 (Panel B). Data are mean ± S.D. (n = 3).

Figure 4: x-z planar LSCM images taken at 48 h after the administration of 16-NBD (green) labeled SLN and NLC aqueous suspensions, Noveon® AA-1 hydrogels, Pluronic-F127 hydrogels and fibrin-based scaffolds.

Figure 5: x-z planar LSCM images taken at 48 h after the administration of NR (red) labeled SLN and NLC aqueous suspensions aqueous suspensions, Noveon® AA-1 hydrogels, Pluronic-F127 hydrogels and fibrin-based scaffolds. The white circle illustrates the dye penetration into the skin.

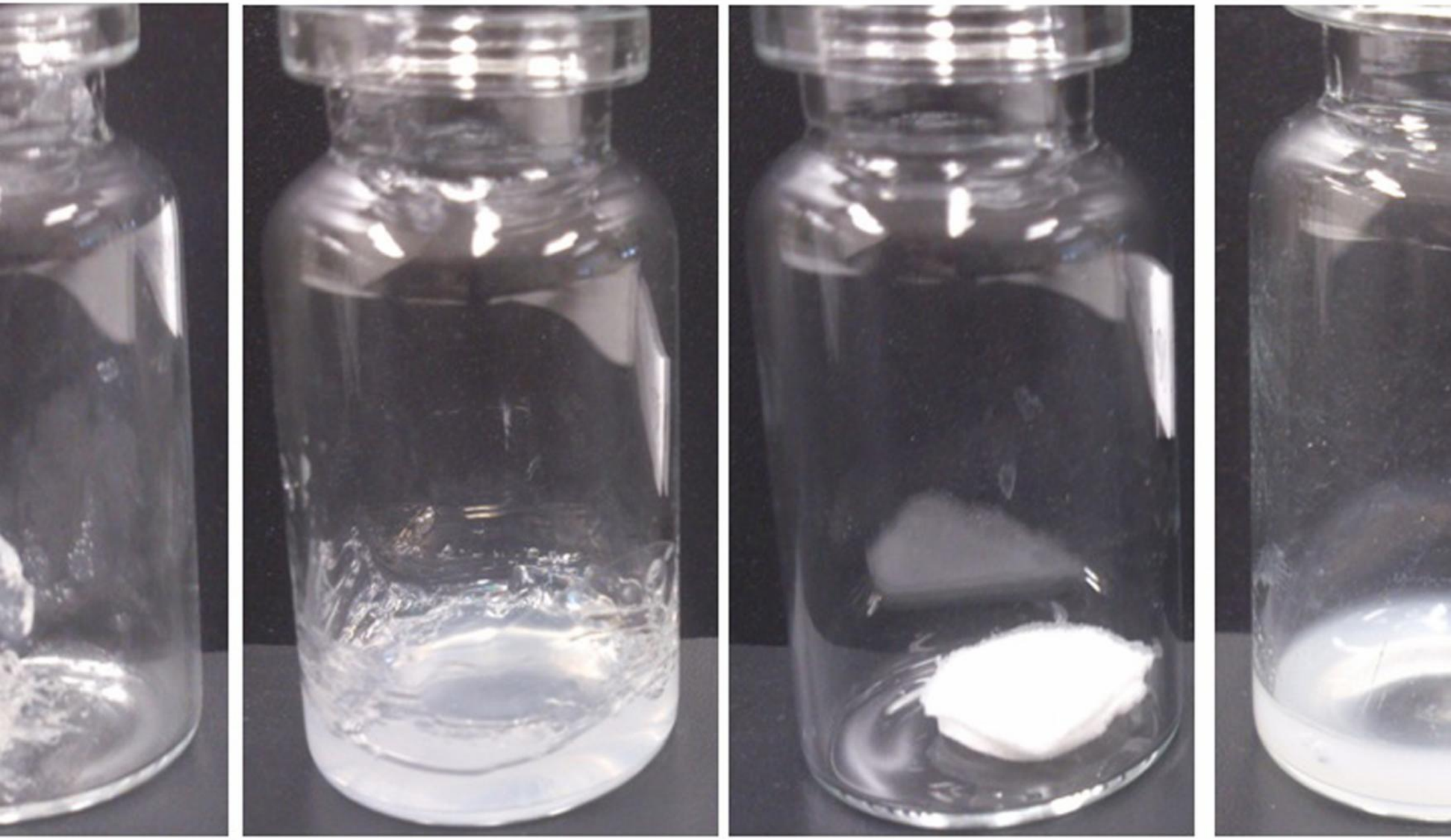

eon® AA-1
ogel

NP in Pluronic F-127
hydrogel

NP in Fibrin-based
scaffold

Reconst
suspe

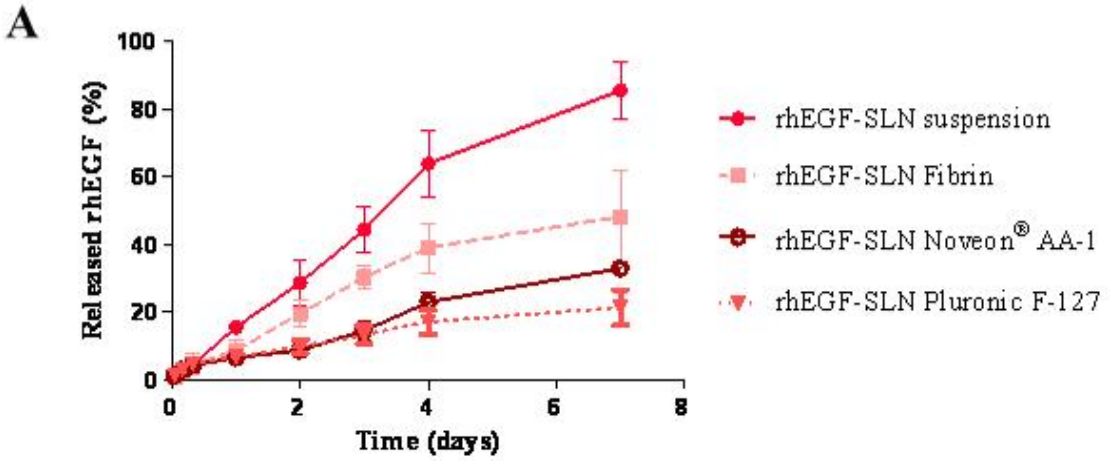
A
Released rhEGF (%)
100
80
60
40
20
0
0
2
4
6
8
Time (days)
rhEGF-SLN suspension
rhEGF-SLN Fibrin
rhEGF-SLN Noveon® AA-1
rhEGF-SLN Pluronic F-127

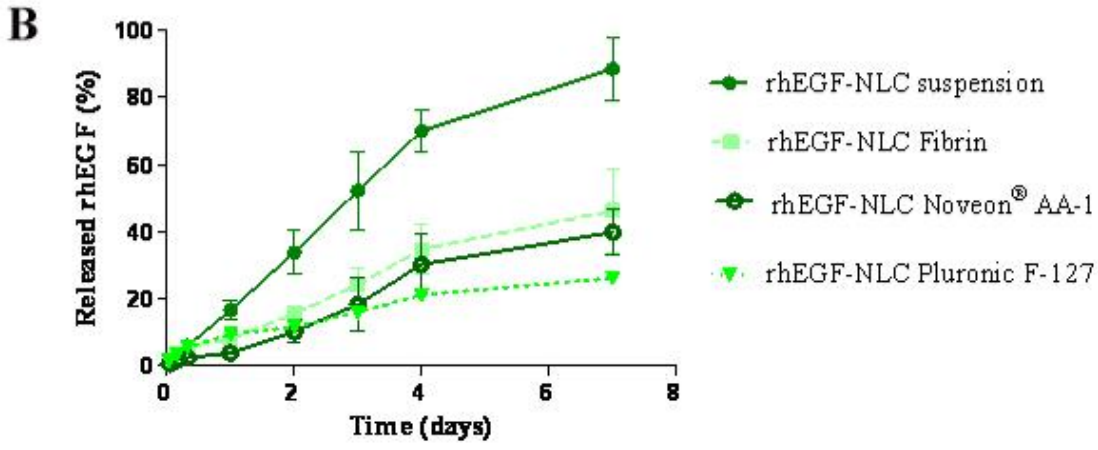
B
Released rhEGF (%)
100
80
60
40
20
0
0
2
4
6
8
Time (days)
rhEGF-NLC suspension
rhEGF-NLC Fibrin
rhEGF-NLC Noveon® AA-1
rhEGF-NLC Pluronic F-127

A

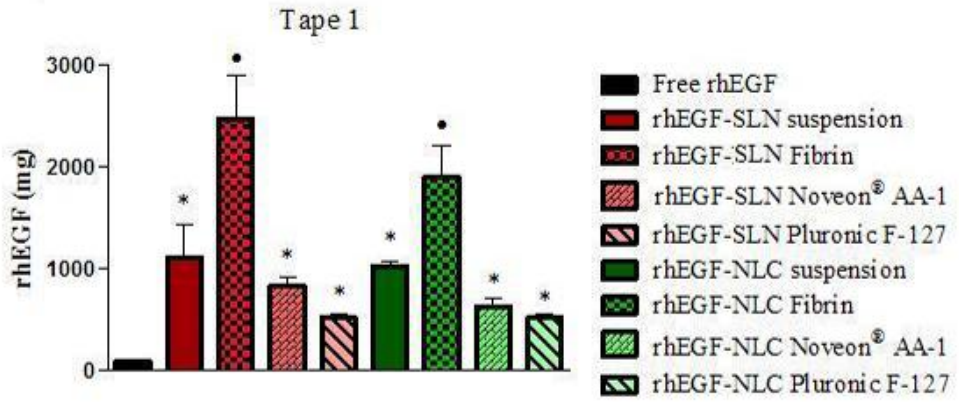
Tape 1
rhEGF (mg)
3000
2000
1000
0
*
Free rhEGF
rhEGF-SLN suspension
rhEGF-SLN Fibrin
rhEGF-SLN Noveon® AA-1
rhEGF-SLN Pluronic F-127
rhEGF-NLC suspension
rhEGF-NLC Fibrin
rhEGF-NLC Noveon® AA-1
rhEGF-NLC Pluronic F-127

B

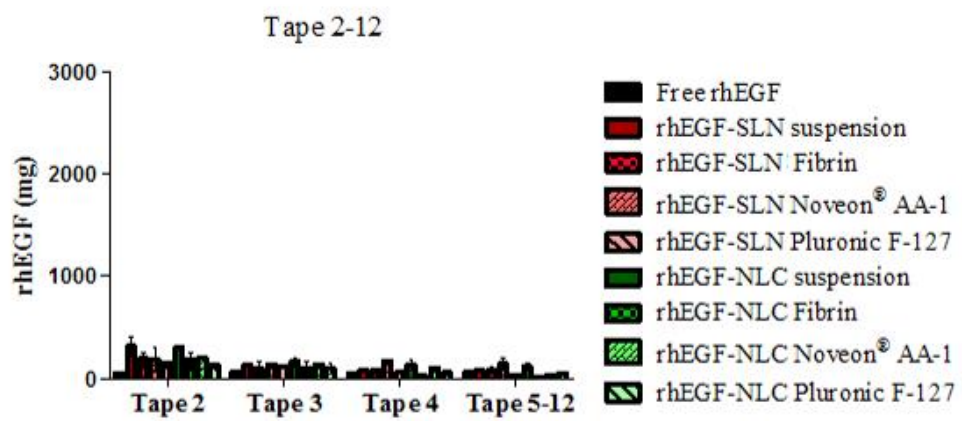
Tape 2-12
rhEGF (mg)
3000
2000
1000
0
Tape 2
Tape 3
Tape 4
Tape 5-12
Free rhEGF
rhEGF-SLN suspension
rhEGF-SLN Fibrin
rhEGF-SLN Noveon® AA-1
rhEGF-SLN Pluronic F-127
rhEGF-NLC suspension
rhEGF-NLC Fibrin
rhEGF-NLC Noveon® AA-1
rhEGF-NLC Pluronic F-127

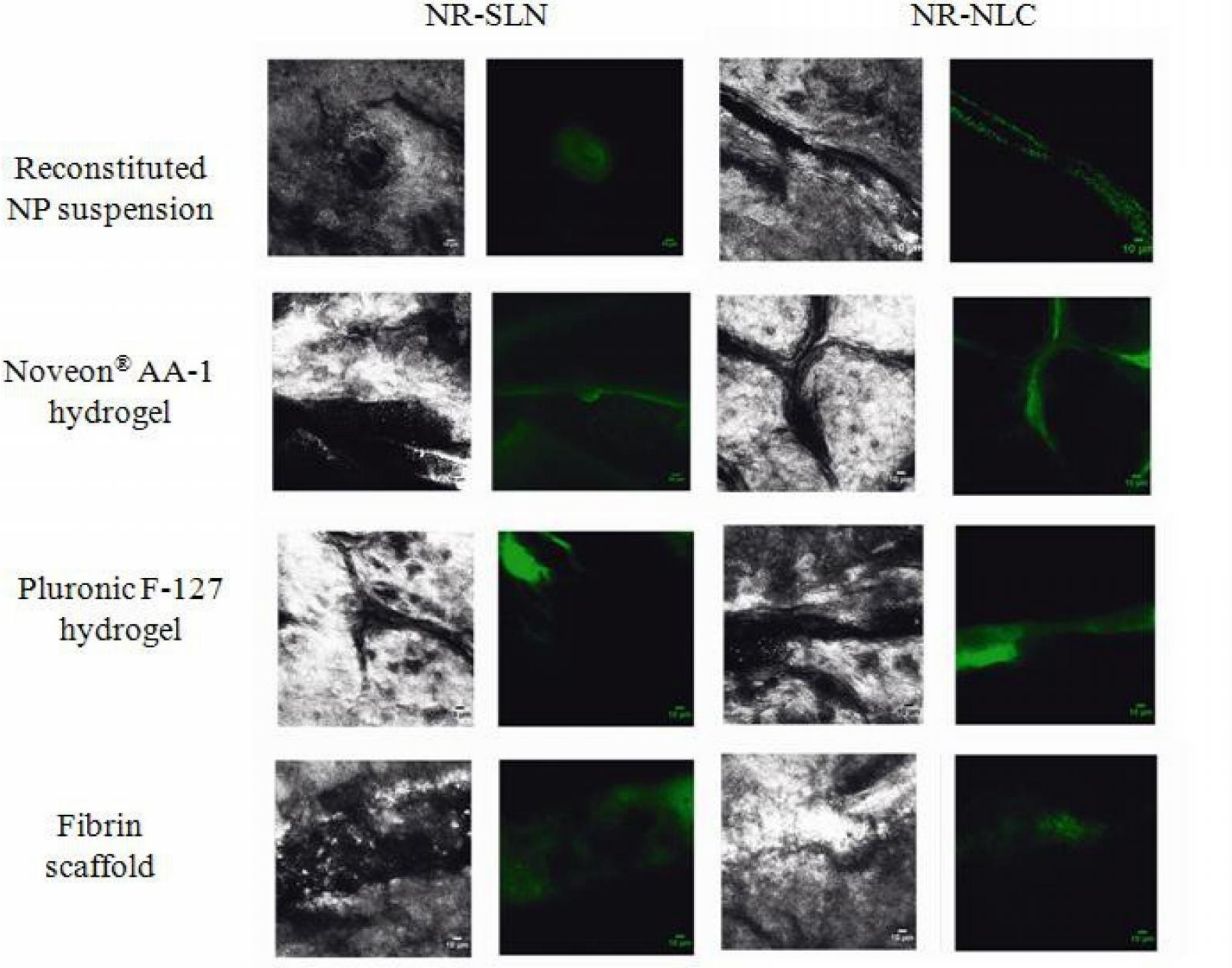
NR-SLN
NR-NLC
Reconstituted NP suspension
Noveon® AA-1 hydrogel
Pluronic F-127 hydrogel
Fibrin scaffold

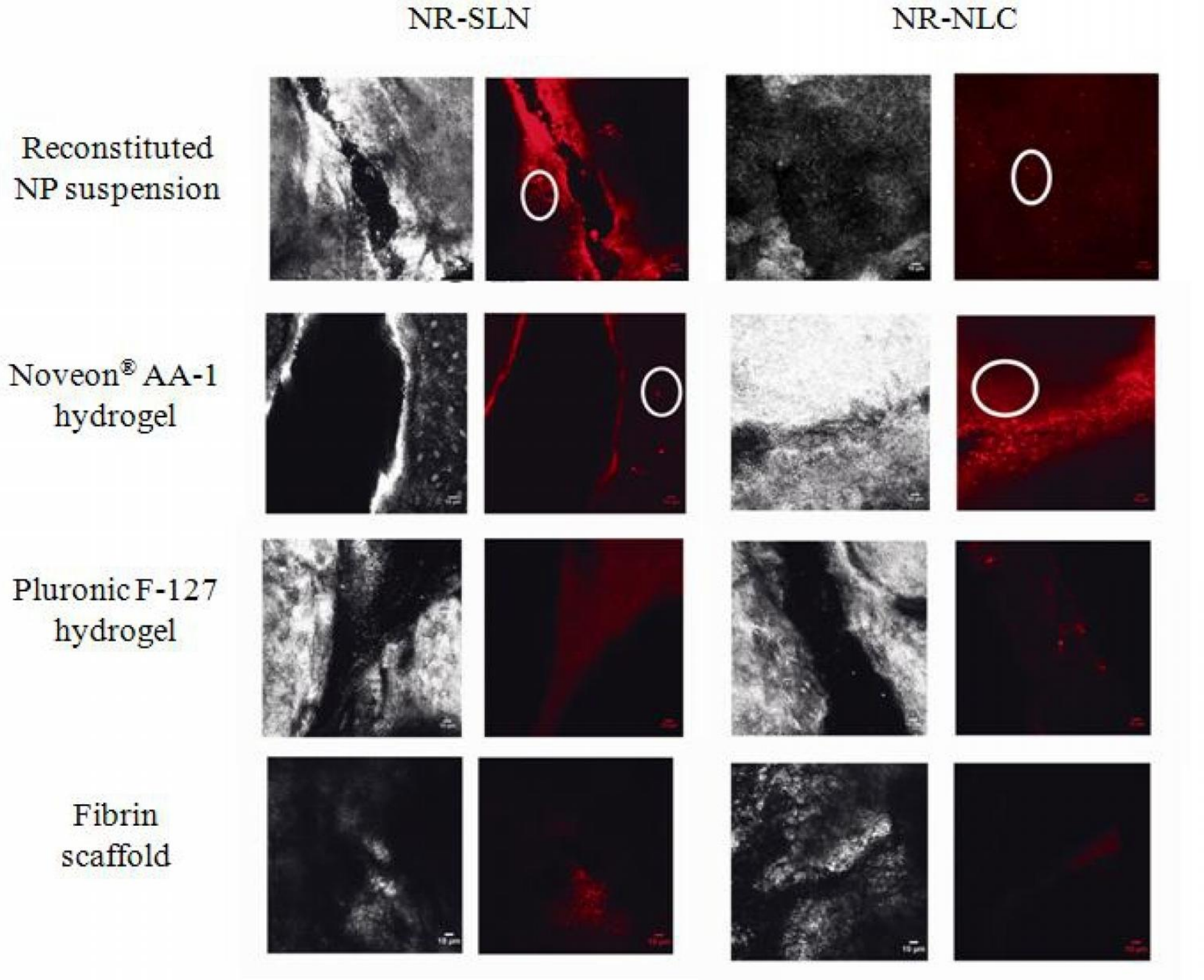
NR-SLN
NR-NLC
Reconstituted NP suspension
Noveon® AA-1 hydrogel
Pluronic F-127 hydrogel
Fibrin scaffold